This article was downloaded by: [Renmin University of China]
On: 13 October 2013, At: 10:51
Publisher: Taylor & Francis
Informa Ltd Registered in England and Wales Registered Number: 1072954 Registered office: Mortimer House, 37-41 Mortimer Street, London W1T 3JH, UK

Journal of Coordination Chemistry
Publication details, including instructions for authors and subscription information:
http://www.tandfonline.com/loi/gcoo20

Synthesis and conductivity of hybrid materials based on germanium-containing polyoxometalates and ionic liquids

NAIQIN TIAN [a] , XIA TONG [a] , HAORUI GU [a] , QINGYIN WU [a] & WENFU YAN [b]

[a] Department of Chemistry , Zhejiang University , Hangzhou , China

[b] State Key Laboratory of Inorganic Synthesis and Preparative Chemistry , Jilin University , Changchun , China

Accepted author version posted online: 11 Dec 2012.Published online: 29 Jan 2013.

To cite this article: NAIQIN TIAN , XIA TONG , HAORUI GU , QINGYIN WU & WENFU YAN (2013) Synthesis and conductivity of hybrid materials based on germanium-containing polyoxometalates and ionic liquids, Journal of Coordination Chemistry, 66:3, 379-384, DOI: 10.1080/00958972.2012.757601

To link to this article: http://dx.doi.org/10.1080/00958972.2012.757601

PLEASE SCROLL DOWN FOR ARTICLE

Taylor & Francis makes every effort to ensure the accuracy of all the information (the "Content") contained in the publications on our platform. However, Taylor & Francis, our agents, and our licensors make no representations or warranties whatsoever as to the accuracy, completeness, or suitability for any purpose of the Content. Any opinions and views expressed in this publication are the opinions and views of the authors, and are not the views of or endorsed by Taylor & Francis. The accuracy of the Content should not be relied upon and should be independently verified with primary sources of information. Taylor and Francis shall not be liable for any losses, actions, claims, proceedings, demands, costs, expenses, damages, and other liabilities whatsoever or howsoever caused arising directly or indirectly in connection with, in relation to or arising out of the use of the Content.

This article may be used for research, teaching, and private study purposes. Any substantial or systematic reproduction, redistribution, reselling, loan, sub-licensing, systematic supply, or distribution in any form to anyone is expressly forbidden. Terms &

Journal of Coordination Chemistry
Vol. 66, No. 3, 10 February 2013, 379–384

Synthesis and conductivity of hybrid materials based on germanium-containing polyoxometalates and ionic liquids

NAIQIN TIAN†, XIA TONG†, HAORUI GU†, QINGYIN WU†* and WENFU YAN‡

†Department of Chemistry, Zhejiang University, Hangzhou, China
‡State Key Laboratory of Inorganic Synthesis and Preparative Chemistry, Jilin University, Changchun, China

(*Received 21 August 2012; in final form 11 October 2012*)

Three new compounds, $[MIMPS]_5GeW_{11}VO_{40}$, $[MIMPS]_5GeW_{10}MoVO_{40}$, and $[MIMPS]_5GeMo_{11}VO_{40}$, have been synthesized from 1-(3-sulfonic group) propyl-3-methyl imidazolium (MIMPS, $C_7H_{13}N_2O_3$) and germanium-containing heteropoly acids $H_5GeW_{11}VO_{40}$, $H_5GeW_{10}MoVO_{40}$, and $H_5GeMo_{11}VO_{40}$. IR spectra indicate the formation of the hybrid molecular compounds showing fingerprint vibrational bands of both heteropolyanions and MIMPS cations. The products exhibit high conductivity and small conductive activation energies; conductivities increase with higher temperature. Their conductivities are as follows: $[MIMPS]_5GeW_{11}VO_{40} > [MIMPS]_5GeW_{10}MoVO_{40} > [MIMPS]_5GeMo_{11}VO_{40}$. The sequence is opposite for their conductive activation energies. The results show that the conductivity and conductive activation energies are closely related to their component elements. The W-containing material exhibits higher conductivity and smaller conductive activation energy than Mo-containing material.

Keywords: *Polyoxometalate;* Ionic liquid; Quasi-solid-state; Conductivity; Activation energy

1. Introduction

Heteropoly compounds (HPAs), an important kind of solid acid, have attracted interest in catalysis, medicine, biology, and materials science, due to their excellent properties such as simple composition, structure determination, the structural features of both complex and metal-oxide, and acidic oxidation–reduction [1–4]. The design and synthesis of HPA derivatives are of interest for applications in catalysis, medicine, conductivity, and nanotechnology [5,6]. Ionic liquids (ILs) are fluids below the boiling point of water which exhibit properties such as non-volatility, thermodynamic stability, non-flammability, electrical conductivity, and wider electrochemical properties [7–11]. Recently, pairing of HPA and IL generated interesting polyoxometalate-based ionic liquid (POM-IL) materials [12,13]. The polyoxometalates (POMs) retain structures of parent HPAs in the POM-IL materials and show properties of both heteropolyanions and ILs. HPAs based on ILs offer several advantages: solvent-free, zero vapor pressure, residual acidity, good thermal stability, and much higher ionic conductivity than the corresponding anhydrous solid analogs. Studies on POM-IL hybrid materials have progressed rapidly. Giannelis reported a new family of POM based on liquid salts prepared by $PW_{12}O_{40}^{3-}$ and bulky poly(ethylene glycol)-containing quaternary

---

*Corresponding author. Email: qywu@zju.edu.cn

Journal of Coordination Chemistry
ISSN 0095-8972 print/ISSN 1029-0389 online
http://dx.doi.org/10.1080/00958972.2012.757601

ammonium cation. The liquid POM derivative has higher conductivity than that of its solid analog, which has been found promising for electrolytes. However, they are still limited to binary POMs, and there are few reports of ternary or quaternary POM-IL hybrid materials. We chose N-methyl imidazolium containing 1-(3-sulfonic group) propyl (MIMPS) and germanium-containing POMs with Keggin structure to synthesize three quasi-solid-state hybrid materials. Their thermal stabilities and conductive performances are ascertained in this study.

2. Experimental

2.1. *Chemicals and instrumentation*

FTIR spectra were recorded on a Nicolet Nexus 470 FT/IR spectrometer from 400–4000 cm^{-1} using KBr pellets. UV spectrum was measured on a SHIMADZU U-2550 UV-vis spectrophotometer. X-ray powder diffraction pattern was obtained on a Bruker D8 Advance X-ray Diffractometer using a Cu tube operated at 40 kV and 40 mA from $2\theta = 5$–40° at a rate of $0.02° s^{-1}$. The thermal stability of the sample was investigated using simultaneous thermogravimetry (TG) and differential thermal analysis (DTA) from room temperature to 800 °C. Measurement was performed using a Shimadzu thermal analyzer in a nitrogen stream with a scanning rate of 10 $°C min^{-1}$. Conductivity measurements of products were measured on a DDS-11A conductivity meter. All reagents were of analysis grade.

2.2. *Synthesis of hybrid materials*

1-(3-sulfonic group) propyl-3-methyl imidazolium (MIMPS, $C_7H_{13}N_2O_3$) was synthesized according to the literature [14]. $H_5GeW_{11}VO_{40}$, $H_5GeW_{10}MoVO_{40}$, and $H_5GeMo_{11}VO_{40}$ were synthesized according to the literatures [15,16]. The presynthesized MIMPS and germanium-containing heteropoly acid were taken in 5 : 1 mol ratio to give one mole of the hybrid material. MIMPS was added to an aqueous solution of HPA (0.2 $g mL^{-1}$), and then the mixture was stirred for 12 h at room temperature. Water was first evaporated in a water bath at 50 °C and then removed in vacuum to give the products which exhibit strong viscosity even quasi-solid-state. The obtained compounds are highly insoluble in tetrahydrofuran, acetone and ethyl acetate, and soluble in dimethylformamide and dimethyl sulfoxide.

3. Results and discussion

3.1. *IR and UV spectra*

Supplementary material shows IR spectra of the POM salts. Vibrations corresponding to HPA with Keggin structure are at 700–1000 cm^{-1}. The vibrational frequencies fall in the sequence of $\nu_{as}(M–O_d) > \nu_{as}(M–O_b–M) > \nu_{as}(Ge–O_a) > \nu_{as}(M–O_c–M)$ (M = W, Mo, V), which are assigned to M–O stretch, stretch of M–O–M bridges between corner-sharing MO_6 octahedral, Ge–O stretch and bending of M–O–M intra bridges between edge-sharing MO_6 octahedra, respectively. There are many characteristic bands of the anion in the IR spectrum of $[MIMPS]_5GeW_{11}VO_{40}$ (curve *a*): 973 cm^{-1}, $\upsilon_{as}(M–O_d)$; 891 cm^{-1},

Table 1. Assignments of the vibrational peaks of the POM salts.

Wavenumber (cm^{-1})			
$[MIMPS]_5GeW_{11}VO_{40}$	$[MIMPS]_5GeMoW_{10}V_{40}$	$[MIMPS]_5GeMo_{11}VO_{40}$	Vibration
3434	3433	3429	O–H stretching
3139	3140	3128	$–CH_2$ stretching
2962	2962	2933	Aliphatic ν(C–H)
1635	1636	1642	H–O–H bending
1571	1566	1560	Imidazole ν(ring stretching)
1462	1462	1462	$–CH_2$ scissoring
1226	1226	1238	S=O stretching
1168	1168	1174	Imidazole H–C–C & H–C–N bending
1048	1048	1048	$–CH_2$ rocking
973	966	955	$M–O_d$ stretching
891	891	880	$M–O_b–M$ stretching
829	822	805	$Ge–O_a$ stretching
782	782	776	$M–O_c–M$ bending
621	621	614	Imidazole $C_2–N_1–C_5$ bending

$\upsilon_{as}(M–O_b–M)$; 829 cm^{-1}, $\upsilon_{as}(Ge–O_a)$; 782 cm^{-1}, $\upsilon_{as}(M–O_c–M)$. The similarities of the spectra of $[MIMPS]_5GeW_{10}MoVO_{40}$ (curve *b*) and $[MIMPS]_5GeMo_{11}VO_{40}$ (curve *c*) with $[MIMPS]_5GeW_{11}VO_{40}$ strongly indicates that they have the same structure as $GeM_{12}O_{40}^{5-}$, showing that they still maintain Keggin structure after introduction of other atoms, which coincide with those reported in the literature for a Keggin unit [17]. In comparison with the parent anion $[\alpha\text{-}GeW_{11}O_{39}]^{8-}$, the $\upsilon_{as}(M–O_d)$ vibration frequencies have red shifts. The major reason may be that the ions have stronger interactions to terminal oxygens of polyoxoanions, impairing the $M–O_d$ bond, reducing the $M–O_d$ force constant, and leading to a decrease in the $M–O_d$ vibration frequency [18]. Assignments of the vibrational peaks of the hybrid materials are shown in table 1. Bands corresponding to both organic cations and inorganic anions can be easily identified and confirm the formation of the hybrid molecular compounds. There are characteristic peaks at 1226–1238 cm^{-1} (S=O), 1048, 1462 ($V_{C–H}$ of CH_2), and 1560–1571 cm^{-1} (imidazole ring) of MIMPS cation, showing the existence of Keggin units in the compounds without depolymerization or degradation.

The absorption of the HPA UV spectrum shows the charge transfer between oxygen and a metal. UV spectra of the POM salts are provided in supplementary material. Absorption spectra of $[MIMPS]_5GeW_{11}VO_{40}$ and $[MIMPS]_5GeW_{10}MoVO_{40}$ in curves *a* and *b* display intense absorptions at 202 and 201 nm (O→M) and relatively weak absorptions at 264 and 267 nm, respectively. However, an intense absorption at 206 nm and two broad shoulders at 248 and 310 nm in curve *c* were caused by charge–transfer of the terminal oxygen and bridge-oxygen to metal in the UV spectrum. The results coincide with those reported for pure heteropoly acids, indicating that the hybrid materials still maintain Keggin structure after introduction of MIMPS cations.

3.2. *X-ray diffraction (XRD) pattern*

The phase and structure of the POM salts are further identified by using powder XRD (Supplementary material). The intense peaks in the PXRD pattern of hybrid materials appear at $2\theta = 8.66°$, $8.57°$, and $8.92°$, respectively, which are characteristic peaks of Keggin structure for $2\theta = 7–11°$ [19]. The XRD pattern at $2\theta = 12–40°$ of the hybrid materials is consistent with the liquid-state nature of the samples [20]. The phase change of the hybrid molecular compounds was caused by the replacement of protons in HPA with MIMPS cations [21]. Moreover, the diffraction patterns contain a strong fundamental reflection in the small-angle region, which arises from the regular arrangement of molecules in layers [22]. These results indicate that these compounds have a layered type of structure. Meanwhile, a broad diffraction peak appears at $2\theta = 25.80°$ in the wide-angle region, indicating that a smectic phase exists [23].

3.3. *TG and DTA curves*

TG and DTA curves of the POM salts are given in supplementary material. The initial low-temperature TG losses from 80–150 °C are due to small amounts of water present in the samples. The TG curves show that the total weight losses of $[\mathrm{MIMPS}]_5\mathrm{GeW}_{11}\mathrm{VO}_{40}$, $[\mathrm{MIMPS}]_5\mathrm{GeW}_{10}\mathrm{MoVO}_{40}$, and $[\mathrm{MIMPS}]_5\mathrm{GeMo}_{11}\mathrm{VO}_{40}$ are 4.01, 3.54, and 6.23 wt.%, indicating that 8.89, 7.63, and 10.58 waters are lost, respectively. The second weight losses are primarily due to the decomposition of MIMPS. The TG trace of $[\mathrm{MIMPS}]_5\mathrm{GeW}_{11}\mathrm{VO}_{40}$ shows an obvious weight loss of nearly 24.39 wt.% (25.53 wt.% for $[\mathrm{MIMPS}]_5\mathrm{GeW}_{10}\mathrm{MoVO}_{40}$ and 33.54 wt.% for $[\mathrm{MIMPS}]_5\mathrm{GeMo}_{11}\mathrm{VO}_{40}$) between 300 and 650 °C, which correspond to 26.09 wt.% of MIMPS contained in the POM-IL (26.83 wt.% for $[\mathrm{MIMPS}]_5\mathrm{GeW}_{10}\mathrm{MoVO}_{40}$ and 34.08 wt.% for $[\mathrm{MIMPS}]_5\mathrm{GeMo}_{11}\mathrm{VO}_{40}$).

The temperature of the exothermic peak in the DTA curve of HPA is used as a way of charaterizing its thermostability. In the DTA curves, there are both exothermic and endothermic peaks. The process of dehydration of $[\mathrm{MIMPS}]_5\mathrm{GeW}_{11}\mathrm{VO}_{40}$ occurring at 148 °C (150 °C for $[\mathrm{MIMPS}]_5\mathrm{GeW}_{10}\mathrm{MoVO}_{40}$ and 87 °C for $[\mathrm{MIMPS}]_5\mathrm{GeMo}_{11}\mathrm{VO}_{40}$) is endothermic. Exothermic peaks at 388 and 715 °C (396, 709 °C for $[\mathrm{MIMPS}]_5\mathrm{GeW}_{10}\mathrm{MoVO}_{40}$ and 377, 750 °C for $[\mathrm{MIMPS}]_5\mathrm{GeMo}_{11}\mathrm{VO}_{40}$) are due to decomposition of MIMPS and Keggin-type anion, respectively.

3.4. *Conductivity*

Conductivity is an important parameter [24]. We have recorded the conductivity of the POM-IL at different temperatures and specific relative humidity (RH). The conductivity of the products was measured for 6.80×10^{-2}, 3.80×10^{-2}, and $3.00 \times 10^{-3}\,\mathrm{S\,cm^{-1}}$ at 89 °C and 30% RH. For their conductivity, the sequences are: $[\mathrm{MIMPS}]_5\mathrm{GeW}_{11}\mathrm{VO}_{40} > [\mathrm{MIMPS}]_5\mathrm{GeW}_{10}\mathrm{MoVO}_{40} > [\mathrm{MIMPS}]_5\mathrm{GeMo}_{11}\mathrm{VO}_{40}$. Figure 1 shows the conductive Arrhenius plots of the POM salts. From the slope, the conductive activation energy E_a can be evaluated using the relation:

$$\sigma = \sigma_0 \exp\left(\frac{-E_a}{\kappa T}\right) \tag{1}$$

where E_a denotes the conductive activation energy, σ_0 is the preexponential factor, and κ is the Boltzmann constant. We can calculate the conductive activation energies of the hybrid materials, which are $10.00\,\mathrm{kJ\,mol^{-1}}$ ($[\mathrm{MIMPS}]_5\mathrm{GeW}_{11}\mathrm{VO}_{40}$), $17.70\,\mathrm{kJ\,mol^{-1}}$ ($[\mathrm{MIMPS}]_5\mathrm{GeW}_{10}\mathrm{MoVO}_{40}$), and $23.17\,\mathrm{kJ\,mol^{-1}}$ ($[\mathrm{MIMPS}]_5\mathrm{GeMo}_{11}\mathrm{VO}_{40}$), respectively. In the range of measured temperature, their conductivity increase with higher temperature. Table 2 shows conductivity at 89 °C, 30% RH, and activation energies of

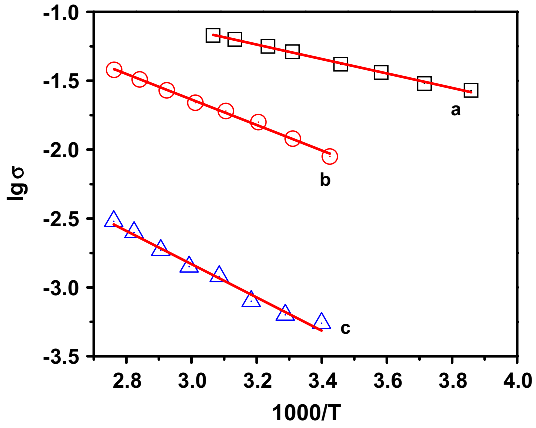

Figure 1. The conductive Arrhenius plots of the POM salts, $[MIMPS]_5GeW_{11}VO_{40}$ (a); $[MIMPS]_5GeW_{10}MoVO_{40}$ (b); $[MIMPS]_5GeMo_{11}VO_{40}$ (c).

Table 2. The conductivity at 89 °C, 30% RH, and activation energies of ion conduction of the hybrid materials.

Samples	Conductivity ($\times 10^{-2}$ S cm^{-1})	Activation energies of proton conduction
$[MIMPS]_5GeW_{11}VO_{40}$	6.80	10.00
$[MIMPS]_5GeMoW_{10}VO_{40}$	3.80	17.70
$[MIMPS]_5GeMo_{11}VO_{40}$	0.30	23.17

ion conduction of the hybrid materials. The results show that conductivity and conductive activation energies are closely related to their component elements. The W-containing material exhibits higher conductivity and smaller conductive activation energy than Mo-containing material.

4. Conclusions

We have reported the syntheses and conductive preformances of materials based on germanium-containing POMs and ILs. The products exhibit strong viscosity and even are quasi-solid. They have high conductivity and small conductive activation energies. The sequence is opposite for their conductive activation energies. This work lays the foundation for research and development of POM-IL hybrid materials.

Acknowledgements

This work was funded by the National Nature Science Foundation of China (21071124, 21173189), the Foundation of NSFC-RFBR (21211120160), the Foundation of State Key Laboratory of Inorganic Synthesis and Preparative Chemistry of Jilin University (2013-06), the Foundation of National Student Research Program, and SRTP Foundation of Zhejiang University (201210335026).

References

[1] Y. Shen, J. Peng, H.Q. Zhang, X. Yu, A.M. Bond. *Inorg. Chem.*, **51**, 5146 (2012).

[2] X. Tong, X.F. Wu, Q.Y. Wu, W.M. Zhu, F.H. Cao, W.F. Yan. *Dalton Trans.*, **41**, 9893 (2012).

[3] J. Wu, C.X. Wang, K. Yu, Z.H. Su, Y. Yu, B.B. Zhou. *J. Coord. Chem.*, **65**, 69 (2012).

[4] X. Tong, W.M. Zhu, Q.Y. Wu, X.Y. Qian, Z. Liu, W.F. Yan, J. Gong. *J. Alloys Compd.*, **509**, 7768 (2011).

[5] K. Kamata, Y. Sumida, K. Yamaguchi, S. Hikichi, N. Mizuno. *Science*, **300**, 964 (2003).

[6] P.E. Car, M. Guttentag, K.K. Baldridge, R. Alberto, G.R. Patzke. *Green Chem.*, **14**, 1680 (2012).

[7] X.Q. Sun, H.M. Luo, S. Dai. *Chem. Rev.*, **112**, 2100 (2012).

[8] L. Timperman, H. Galiano, D. Lemordant, M. Anouti. *Electrochem. Commun.*, **13**, 1112 (2011).

[9] P. Hapiot, C. Lagrost. *Chem. Rev.*, **108**, 2238 (2008).

[10] K. Tanabe, Y. Suzui, M. Hasegawa, T. Kato. *J. Am. Chem. Soc.*, **134**, 5652 (2012).

[11] G. Rangits, Z. Berente, T. Kegl, L. Kollar. *J. Coord. Chem.*, **58**, 869 (2005).

[12] R.Y. Wang, D.Z. Jia, Y.L. Cao. *Electrochim. Acta*, **72**, 101 (2012).

[13] Z. Nadealian, V. Mirkhani, B. Yadollahi, M. Moghadam, S. Tangestaninejad, I. Mohammadpoor-Baltork. *J. Coord. Chem.*, **65**, 1071 (2012).

[14] Y. Leng, J. Wang, D.R. Zhu, X.Q. Ren, H.Q. Ge, L. Shen. *Angew. Chem. Int. Ed.*, **48**, 168 (2009).

[15] X.G. Sang, Q.Y. Wu. *Rare Met.*, **23**, 296 (2004).

[16] Q.Y. Wu, X.G. Sang. *Mater. Res. Bull.*, **40**, 405 (2005).

[17] M. Ammam, J. Fransaer. *J. Solid State Chem.*, **184**, 818 (2011).

[18] J. Miao, S.X. Zhang, S.J. Li, Y.H. Gao, X. Zhang, X.N. Wang, S.X. Liu. *J. Coord. Chem.*, **64**, 4006 (2011).

[19] S.X. Xu, X.F. Wu, Q.Y. Wu, W.F. Yan. *Chin. Sci. Bull.*, **56**, 2679 (2011).

[20] A.B. Bourlinos, K. Raman, R. Herrera, Q. Zhang, L.A. Archer, E.P. Giannelis. *J. Am. Chem. Soc.*, **126**, 15358 (2004).

[21] W.L. Huang, W.S. Zhu, H.M. Li, H. Shi, G.P. Zhu, H. Liu, G.Y. Chen. *Ind. Eng. Chem. Res.*, **49**, 8998 (2010).

[22] Y.X. Jiang, S.X. Liu, S.J. Li, J. Miao, J. Zhang, L.X. Xu. *Chem. Commun.*, **47**, 10287 (2011).

[23] X.K. Lin, W. Li, J. Zhang, H. Sun, Y. Yan, L.X. Wu. *Langmuir*, **26**, 13201 (2010).

[24] M.L. Wei, H.H. Li, G.J. He. *J. Coord. Chem.*, **64**, 4318 (2011).